ISSN: 2476-230X

Research Article

Cardiology: Open Access

Structural Rationale for Impaired Action Regulation by the Cardiomyopathy-Associated R975W Metavinculin Variant: A Short Computational Communication

Aayush Ojha*

Department of Chemistry, University of Maine, USA

***Corresponding Author**
Aayush Ojha, Department of Chemistry, University of Maine, USA.

Submitted: 2026, May 11; **Accepted:** 2026, Jun 08; **Published:** 2026, Jun 15

Citation: Ojha, A. (2026). Structural Rationale for Impaired Action Regulation by the Cardiomyopathy-Associated R975W Metavinculin Variant: A Short Computational Communication. *Cardio Open, 11*(1), 01-09.

Abstract

Background: *Cardiomyopathy-associated variants in the metavinculin-specific tail insert, including A934V, ΔL954, and R975W, have been linked to defective regulation of vinculin-mediated F-actin assembly, but the molecular basis by which individual variants perturb mechanotransduction remains incompletely resolved.*

Purpose: *This short computational communication focuses on R975W and frames it as a testable structural hypothesis for impaired metavinculin-actin regulation.*

Methods: *A preliminary PyMOL-based structural comparison was used to inspect the wild-type metavinculin tail domain and an R975W mutant model, with attention to side-chain chemistry, surface shape, hydrophobicity, and the local actin-regulatory region. The observation was then interpreted using published work on vinculin/metavinculin actin organization, cardiomyopathy-linked metavinculin variants, force-sensitive vinculin-actin binding, molecular dynamics, and single-molecule force spectroscopy.*

Results: *Replacement of Arg 975 with tryptophan removes a positively charged guanidinium-containing side chain and introduces a bulky aromatic hydrophobic residue. Qualitative visualization suggests a local surface protrusion and increased hydrophobicity at the mutation site.*

Conclusion: *R975W provides a plausible structural perturbation that may alter metavinculinactin geometry and weaken force-dependent regulation under cyclic cardiac load. Quantitative molecular dynamics, enhanced sampling, and single-molecule force spectroscopy are needed to test this mechanism.*

Keywords: Vinculin, Mechanotransduction, PyMOL, Molecular Modeling, Catch Bond, Force Spectroscopy

1. Introduction

Familial cardiomyopathies comprise inherited myocardial disorders in which genetic variation can impair contractile performance, force transmission, and long-term cardiac remodeling. Dilated, hypertrophic, and restrictive cardiomyopathy phenotypes differ clinically, but all can involve defects in the molecular systems that allow cardiomyocytes to tolerate repeated mechanical stress [1,2]. Among these systems, vinculin and its muscle enriched splice isoform metavinculin are central because they connect adhesion complexes to filamentous actin and help stabilize cell-cell and cell-matrix junctions during contraction [3,4]. In cardiac tissue, these proteins are concentrated at structures such as intercalated discs and costameres, where mechanical continuity between sarcomeres, membranes, extracellular matrix, and neighboring cells is required for synchronized force transmission [5,6]. Vinculin is a modular cytoskeletal protein whose tail domain binds F-actin and contributes to actin filament organization. Structural and biochemical studies have shown that vinculin can associate with different actin architectures and can support filament bundling when appropriately activated [7-9]. Metavinculin shares the major vinculin architecture but contains an additional 68-residue insert in the actin binding tail domain. This insertion

makes metavinculin more than a larger version of vinculin: it changes how the tail engages actin, limits the bundling behavior typical of vinculin, and has been proposed to tune cytoskeletal stiffness in muscle cells [10-12]. In this view, vinculin provides robust linkage and reinforcement, whereas metavinculin provides a regulatory counterweight that prevents excessive rigidification of actin assemblies during repetitive deformation of the beating heart [13-15].

The mechanical nature of vinculin-actin interaction has recently become a major focus. Computational and experimental work suggests that vinculin-actin binding is not merely a static affinity event but a directional, force-dependent interaction in which bond lifetime can increase under moderate load and then decrease at higher load [16,17]. This catch-bond-like behavior provides a plausible molecular basis for how adhesion proteins can strengthen under physiologically relevant tension. Earlier computational studies also indicated that the vinculin-actin interface involves orientation-dependent contacts and force-sensitive conformational changes [18]. Because metavinculin is closely related to vinculin but has a distinct tail insertion, cardiomyopathy-linked metavinculin variants may perturb not only equilibrium actin binding but also the mechanical response of the protein-actin interface under directional cardiac forces. Several cardiomyopathy-associated metavinculin variants, including A934V, ΔL954, and R975W, map to the metavinculin-specific tail region. Experimental work has shown that these variants can disrupt the ability of metavinculin to regulate vinculin-induced F-actin assemblies, causing abnormal linear bundles and higher-order actin structures rather than normal modulation of actin architecture [11,19]. This finding is important because it suggests that disease-associated metavinculin variants may not simply abolish actin binding. Instead, they may convert metavinculin from a mechanical regulator into a defective modulator that fails to restrain vinculin-driven cytoskeletal stiffening. Such behavior is consistent with the broader concept that protein interaction networks in mechanobiology depend on force-sensitive binding, geometry, and allostery rather than on binding affinity alone [13,20,21].

The present short communication focuses on the R975W variant. Arg975 is chemically distinct from tryptophan: arginine is long, positively charged, and capable of forming electrostatic and hydrogen-bonding interactions, whereas tryptophan is bulky, aromatic, and strongly hydrophobic.

A substitution of this kind can change local side-chain packing, solvent exposure, surface charge, hydrophobicity, and the shape of a protein-protein interaction surface. Using the preliminary PyMOL analysis developed from the original proposal work, this manuscript reframes the result as a conservative, publication-style molecular hypothesis. The goal is not to overinterpret a static model, but to identify why R975W is a structurally plausible perturbation and how that perturbation can be tested by more rigorous computational and single-molecule methods.

2. Methodology / Materials and Methods

The starting structural model was the metavinculin tail domain structure used in the preliminary PyMOL analysis, with emphasis on the R975 site in the metavinculin-specific region. The wildtype model and the R975W mutant model were visualized in PyMOL. The mutation was introduced by replacing arginine with tryptophan at residue 975, followed by qualitative inspection of the local surface, side-chain volume, hydrophobicity, and overall surface contour. The analysis was intentionally restricted to structural visualization and hypothesis generation. No molecular dynamics, minimization-dependent energy ranking, binding free-energy calculation, or experimental force measurement was performed in this preliminary work. The literature was then used to place this structural observation into a mechanobiological framework. Studies of cardiomyopathy genetics and disease phenotypes were used to define clinical relevance [1,2]. Studies on vinculin structure, localization, and actin binding were used to define the baseline cytoskeletal role of the vinculin/metavinculin family [3,4,7-9]. Structural and biochemical studies of metavinculin were used to interpret the significance of the metavinculin-specific insert [10-12,15]. Recent work on force sensitive vinculinactin binding and mechano transduction was used to build a testable model for force-dependent impairment [14,16-18]. Finally, methodological literature on molecular dynamics, steered molecular dynamics, enhanced sampling, and single-molecule force spectroscopy was used to define how the hypothesis should be validated [22-34]. Because the present work is a short communication based on preliminary modeling, the central output is a structurally constrained hypothesis rather than a definitive mechanism. The proposed interpretation is therefore stated in probabilistic language throughout the manuscript.

2.1. Statistical Analysis

No statistical analysis was performed because this short communication reports a qualitative structural visualization and hypothesis-generating interpretation rather than a new experimental dataset.

2.2. Ethical Approval

Ethical approval was not required because the work used publicly available structural information and did not involve human participants, animals, or newly collected clinical specimens.

3. Results / Findings

3.1. R975W Produces a Chemically Severe Local Substitution in the Metavinculin Tail

The PyMOL comparison indicates that R975W introduces two visually apparent changes in the metavinculin tail domain: a local surface protrusion and an increased hydrophobic patch at the mutation site (Figure 1). These changes are chemically plausible consequences of replacing arginine with tryptophan. Arginine contains a flexible aliphatic chain terminated by a positively charged guanidinium group, allowing it to form salt bridges, hydrogen bonds, and solvent mediated interactions. Tryptophan, by contrast, is a bulky aromatic residue with a large indole ring. Even when the protein backbone remains unchanged, this substitution can alter the local surface because the tryptophan side chain occupies more hydrophobic volume and presents a different interaction chemistry

to neighboring residues, solvent, and binding partners. In the context of metavinculin, this change is not trivial. The tail domain is the region through which vinculin and metavinculin interact with actin and regulate filament organization [4]. Metavinculin's68-resi due insert changes the actin-organizing behavior of the tail domain and limits the strong bundling activity associated with vinculin [10,12]. Thus, a mutation that locally changes hydrophobicity and steric shape within this regulatory region could shift the balance between productive actin engagement, steric interference with bundling, and abnormal assembly formation. The observation that cardiomyopathy-associated metavinculin variants fail to inhibit vinculin-mediated F-actin bundling supports this interpretation at the cellular and biochemical level [11,19].

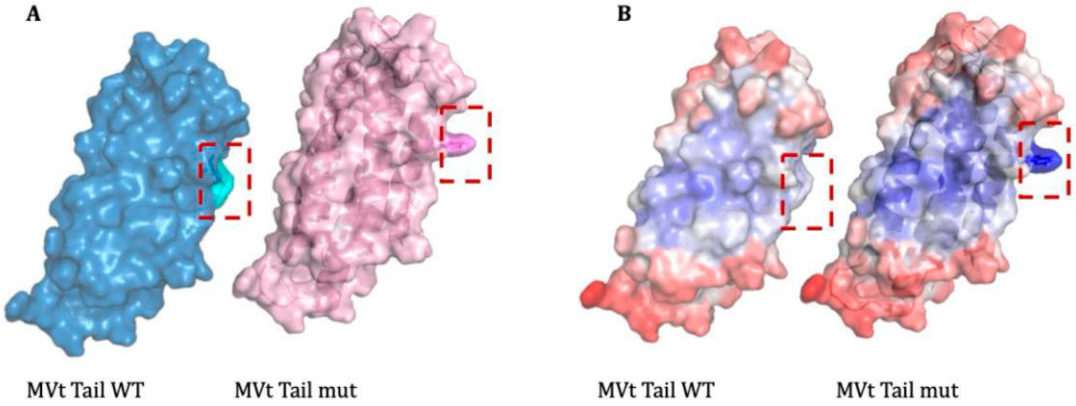

Figure 1: Structural effects of the cardiomyopathy-linked R975W mutation in the metavinculin tail domain. **(A)** Surface comparison of wild-type (left, blue) and R975W mutant (right, pink) metavinculin tail domains (PDB 3MYI). The mutation replaces a positively charged arginine with a bulky hydrophobic tryptophan, producing a noticeable surface protrusion at the mutation site (highlighted in both), which may disturb actin-binding geometry. **(B)** Electrostatic/hydrophobic surface representation of the same structures, colored by hydrophobicity (blue = more hydrophobic; redder = more hydrophilic). The mutant exhibits a more hydrophobic patch at the site of mutation compared with the corresponding surface in the wild-type model.

Evidence Layer	Relevance to the present communication	Key citations
Clinical and genetic context	Cardiomyopathy can arise from inherited defects that impair cardiac mechanical performance and sudden-death risk.	[1,2]
Vinculin family structure and localization	Vinculin/metavinculin connect adhesion sites to actin networks at mechanically loaded cellular structures.	[3-6]
Actin organization	Vinculin promotes actin association and bundling; metavinculin modifies this behavior through its tail insert.	[7-12]
Disease variants	A934V, ΔL954, and R975W can disrupt normal metavinculin control of vinculin-induced F-actin assemblies.	[15,19]
Force-sensitive binding	Vinculin-actin interaction is directionally force sensitive, making static structural changes potentially load-dependent.	[13,16-18]
Computational validation	Molecular dynamics, SMD, reaction-coordinate design, and enhanced sampling can test dynamic stability and free-energy effects.	[22,26-30,32,33]
Experimental validation	Optical tweezers and single-molecule force spectroscopy can measure force-dependent lifetimes and rupture behavior.	[20,21,23-25,31,34,35]

Table 1: Evidence Framework Supporting and Testing the R975W Metavinculin Hypothesis

4. Discussion

4.1. A Surface Perturbation may be Amplified by Mechanical Loading

Static structural differences can become biologically important when they occur in proteins that operate under load. Vinculin and metavinculin do not function in a mechanically neutral environment; they are embedded in adhesion and cytoskeletal structures that experience cyclic forces. Recent single-molecule and computational studies of vinculin-actin binding show that mechanical direction and force magnitude can influence binding lifetime and unbinding pathways [16,17]. This means that a local change in surface chemistry may have effects that are not captured

by simple visual comparison. A residue that appears peripheral in a static model may become important if it alters the path by which force is propagated across the tail domain or if it changes the orientation required for a mechanically stabilized actin-bound state [13,18]. For R975W, the likely perturbation is twofold. First, the loss of positive charge could remove favorable electrostatic or solvent-mediated interactions that help maintain a particular local arrangement. Second, the added aromatic bulk could alter steric complementarity at or near the actin-regulatory surface. Either effect could change the energy landscape of metavinculin-actin interaction. In a force-sensitive system, such a change could shift the unbinding pathway, reduce bond lifetime under physiological tension, or prevent a force-induced conformational state that normally allows metavinculin to regulate cytoskeletal compliance. This proposed mechanism is consistent with the broader idea that mechanotransduction proteins synchronize biochemical interaction networks by coupling force, conformation, and binding lifetime [13,20,21].

4.2. Why this Hypothesis Matters for Cardiomyopathy

Cardiomyopathy-linked metavinculin mutations are clinically relevant because cardiac muscle must repeatedly transmit force without becoming either mechanically unstable or excessively rigid. Vinculin mediated actin bundling can reinforce adhesion complexes, but excessive or improperly regulated bundling may reduce the dynamic compliance needed for repeated contraction and relaxation [3,7,8]. Metavinculin appears to fine-tune this system by modulating vinculin-driven F-actin organization [10,11,15]. Therefore, the disease-relevant question is not only whether R975W binds actin more or less strongly, but whether it disrupts the regulatory role of metavinculin in maintaining the correct stiffness and architecture of the action network. The observation that metavinculin mutants can promote abnormal large assemblies embedded with linear bundles provides an important bridge between molecular structure and cellular mechanics [19]. If R975W changes local surface shape and hydrophobicity, it could favor non-native contacts, disturb normal orientation on F-actin, or reduce the ability of the metavinculin insert to prevent excessive bundling. Such defects would be expected to affect force transmission at costameres and intercalated discs, both of which are essential for maintaining cardiac tissue integrity [5,6,14]. This gives the PyMOL observation a plausible disease context: a local substitution may be amplified through actin architecture into tissue-level mechanical dysfunction.

4.3. A Validation Path from Visualization to Mechanism

Although the PyMOL result is suggestive, static visualization alone is not sufficient for a mechanistic claim. Publication-quality validation would require at least one layer of quantitative computational or experimental support. Molecular dynamics simulations provide the first natural step because they can test whether the R975W side chain remains stable, causes local rearrangement, changes solvent exposure, disrupts contacts, or alters the flexibility of the metavinculin-specific region [26,27]. NAMD or related packages could be used to perform atomistic simulations under physiological ionic conditions [30]. Steered molecular dynamics would then allow direct testing of how force changes unbinding pathways or structural stability, as has been used in other protein ligand and protein-mechanics settings [28,29,32]. Enhanced sampling approaches could strengthen this analysis. Reaction coordinates should be selected carefully because calculated free-energy landscapes depend strongly on the coordinates chosen [22]. For a metavinculin-actin system, useful variables might include displacement parallel and perpendicular to the actin filament, buried surface area, interface contact number, and rotation of the tail domain relative to the filament. OPES/meta dynamics-based methods implemented through PLUMED could be used to estimate free-energy barriers and compare wild-type and R975W landscapes [33]. A reduction in free-energy barrier, loss of a force-stabilized intermediate, or a shift toward an alternative unbinding pathway would provide stronger evidence that R975W changes mechanical stability. Single-molecule force spectroscopy provides the most direct experimental test. Optical tweezer scan measures the life time of individual protein-protein interactions under controlled piconewton scale force [23,34].

Integrated simulation and single-molecule spectroscopy workflows are increasingly used to connect microscopic conformational models with experimentally measured lifetimes and mechanical observables [36]. In a metavinculinactin assay, purified and site-specifically biotinylated metavinculin tail constructs could be attached to beads, while stabilized F-actin is immobilized in a flow cell. Site-specific bio-tinylation using BirA provides a practical route to controlled molecular orientation [25]. The force-dependent bond lifetime could then be measured across a physiologically relevant force range and interpreted using established single-molecule force spectroscopy theory [24,31]. If wild-type metavinculin displays a force-reinforced lifetime profile but R975W shortens lifetimes or abolishes force reinforcement, this would directly support the hypothesis that the mutation impairs mechanotransduction. The relevant force scale should be chosen with care. Forces produced by molecular motors and transmitted through actin-associated complexes are commonly in the piconewton range, and cooperative behavior among myosin motors can generate larger effective mechanical loads [35]. Therefore, a practical validation program should not test only zero-force binding. Instead, it should compare wild-type and R975W metavinculin under a range of directional loads, because the disease mechanism may emerge only under force. This is particularly important for cardiac proteins that experience cyclic mechanical stress rather than static binding conditions.

4.4. Limitations

The present work has important limitations. First, the analysis is qualitative and based on visualization rather than quantitative energy minimization, molecular dynamics, electrostatic potential calculation, solvent-accessible surface area measurement, or binding free-energy estimation. Second, the R975W side-chain conformation may depend on rotamer choice, local relaxation, and the presence or absence of actin. Third, the metavinculin tail domain model does not fully reproduce the crowded and mechanically loaded environment of cardiac adhesion complexes.

Fourth, the relationship between a local surface patch and disease phenotype is indirect and must be tested through protein mechanics, actin-assembly assays, or cellular force transduction measurements. These limitations do not eliminate the value of the observation, but they determine how it should be interpreted. The most defensible conclusion is that R975W creates a plausible structural perturbation in a mechanically important region of metavinculin. This perturbation provides a focused hypothesis for future simulations and single-molecule experiments rather than a completed disease mechanism.

5. Conclusion

The R975W metavinculin variant replaces a positively charged arginine with a bulky hydrophobic tryptophan in the metavinculin tail domain. Preliminary PyMOL visualization suggests that this substitution generates a local hydrophobic patch and surface protrusion. When interpreted alongside published studies of metavinculin-mediated actin regulation, cardiomyopathy-associated metavinculinmutants, and force-sensitive vinculin-actin binding, the observation supports a testable model in which R975W impairs metavinculin's ability to regulate actin architecture under cardiac mechanical load. The next step should be quantitative validation using molecular dynamics, enhanced free-energy sampling, and single-molecule force spectroscopy. A combined approach of this kind would determine whether the static structural perturbation observed here is sufficient to alter the force-dependent binding landscape of metavinculin-actin interaction.

Acknowledgements

The author acknowledges the prior proposal and preliminary PyMOL visualization work that formed the basis for this short communication.

Declarations

Author Contributions

Aayush Ojha: Conceptualization, Methodology, Visualization, Investigation, Writing - original draft, Writing - review and editing.

Data Availability Statement

No new experimental datasets were generated. The structural interpretation is based on publicly available protein structures and preliminary PyMOL visualization. The author should provide the PyMOL session file and mutant model as supplementary material at submission if available. AI

Usage Statement

During the preparation of this work, the author used AI-assisted language editing and formatting support to improve clarity, organization, and manuscript presentation. After using this support, the author reviewed and edited the content as needed and takes full responsibility for the content of the submitted article.

References

1. Bui, Q. M., Ding, J., Hong, K. N., & Adler, E. A. (2023). The genetic evaluation of dilated cardiomyopathy. *Structural Heart,* 7(5), 100200.
2. Eschenhagen, T., & Carrier, L. (2019). Cardiomyopathy phenotypes in human-induced pluripotent stem cell-derived cardiomyocytes—a systematic review. Pflügers *Archiv-European Journal of Physiology, 47*1(5), 755-768.
3. Bays, J. L., & DeMali, K. A. (2017). Vinculin in cell–cell and cell–matrix adhesions. *Cellular and Molecular Life Sciences, 74*(16), 2999-3009.
4. Ziegler, W. H., Liddington, R. C., & Critchley, D. R. (2006). The structure and regulation of vinculin. *Trends in cell biology, 16*(9), 453-460.
5. Belkin, A. M., Zhidkova, N. I., & Koteliansky, V. E. (1986). Localization of talin in skeletal and cardiac muscles. *FEBS letters, 200*(1), 32-36.
6. Tornavaca, O., Chia, M., Dufton, N., Almagro, L. O., Conway, D. E., Randi, A. M., ... & Balda, M. S. (2015). ZO-1 controls endothelial adherens junctions, cell–cell tension, angiogenesis, and barrier formation. *Journal of Cell Biology, 208*(6), 821-838.
7. Boujemaa-Paterski, R., Martins, B., Eibauer, M., Beales, C. T., Geiger, B., & Medalia, O. (2020). Talin-activated vinculin interacts with branched actin networks to initiate bundles. *Elife*, 9, e53990.
8. Le Clainche, C., Dwivedi, S. P., Didry, D., & Carlier, M. F. (2010). Vinculin is a dually regulated actin filament barbed end-capping and side-binding protein. *Journal of Biological Chemistry, 285*(30), 23420-23432.
9. Shi, B., Matsui, T., Qian, S., Weiss, T. M., Nicholl, I. D., Callaway, D. J., & Bu, Z. (2023). An ensemble of cadherin-catenin-vinculin complex employs vinculin as the major F-actin binding mode. *Biophysical Journal, 122*(12), 2456-2474.
10. Janssen, M. E., Liu, H., Volkmann, N., & Hanein, D. (2012). The C-terminal tail domain of metavinculin, vinculin's splice variant, severs actin filaments. *Journal of Cell Biology, 197(*5), 585-593.
11. Kim, L. Y., Thompson, P. M., Lee, H. T., Pershad, M., Campbell, S. L., & Alushin, G. M. (2016). The structural basis of actin organization by vinculin and metavinculin. *Journal of molecular biology, 428*(1), 10-25.
12. Rangarajan, E. S., & Izard, T. (2021). The cryogenic electron microscopy structure of the cell adhesion regulator metavinculin reveals an isoform-specific kinked helix in its cytoskeleton binding domain. *International Journal of Molecular Sciences, 22*(2), 645.
13. Goult, B. T., von Essen, M., & Hytönen, V. P. (2022). The mechanical cell–the role of force dependencies in synchronising protein interaction networks. *Journal of cell science, 135(22)*, jcs259769.
14. Kanoldt, V., Kluger, C., Barz, C., Schweizer, A. L., Ramanujam, D., Windgasse, L., ... & Grashoff, C. (2020). Metavinculin modulates force transduction in cell adhesion sites. *Nature communications, 11*(1), 6403.
15. Witt, S., Zieseniss, A., Fock, U., Jockusch, B. M., & Illenberger, S. (2004). Comparative biochemical analysis suggests that vinculin and metavinculin cooperate in muscular adhesion sites. *Journal of Biological Chemistry, 279*(30), 31533-31543.

16. Peña Ccoa, W. J., Mukadum, F., Ramon, A., Stirnemann, G., & Hocky, G. M. (2025). A direct computational assessment of vinculin–actin unbinding kinetics reveals catch-bonding behavior. *Proceedings of the National Academy of Sciences, 122*(21), e2425982122.
17. Chirasani, V. R., Khan, M. A. I., Malavade, J. N., Dokholyan, N. V., Hoffman, B. D., & Campbell, S. L. (2023). Molecular basis and cellular functions of vinculin-actin directional catch bonding. *Nature communications, 14*(1), 8300.
18. Golji, J., & Mofrad, M. R. (2013). The interaction of vinculin with actin. *PLoS computational biology, 9*(4), e1002995.
19. Sarker, M., Lee, H. T., Mei, L., Krokhotin, A., de Los Reyes, S. E., Yen, L., ... & Campbell, S. L. (2019). Cardiomyopathy mutations in metavinculin disrupt regulation of vinculin-induced F-actin assemblies. *Journal of molecular biology,* 431(8), 1604-1618.
20. Fritzsche, M. (2020). Thinking multi-scale to advance mechanobiology. *Communications Biology, 3*(1), 469.
21. Nathwani, B., Shih, W. M., & Wong, W. P. (2018). Force spectroscopy and beyond: innovations and opportunities. *Biophysical journal, 115*(12), 2279-2285.
22. Best, R. B., & Hummer, G. (2005). Reaction coordinates and rates from transition paths. *Proceedings of the National Academy of Sciences, 102*(19), 6732-6737.
23. Bustamante, C. J., Chemla, Y. R., Liu, S., & Wang, M. D. (2021). Optical tweezers in single-molecule biophysics. *Nature Reviews Methods Primers*, *1*(1), 25.
24. Dudko, O. K., Hummer, G., & Szabo, A. (2008). Theory, analysis, and interpretation of single-molecule force spectroscopy experiments. *Proceedings of the National Academy of Sciences, 105*(41), 15755-15760.
25. Fairhead, M., & Howarth, M. (2014). Site-specific biotinylation of purified proteins using BirA. In Site-Specific Protein Labeling: Methods and Protocols (pp. 171-184). New York, NY: *Springer New York.*
26. Hollingsworth, S. A., & Dror, R. O. (2018). Molecular dynamics simulation for all. *Neuron, 99*(6), 1129-1143.
27. Karplus, M., & Petsko, G. A. (1990). Molecular dynamics simulations in biology. *Nature, 347*(6294), 631-639.
28. Mykuliak, V. V., Sikora, M., Booth, J. J., Cieplak, M., Shalashilin, D. V., & Hytönen, V. P. (2020). Mechanical unfolding of proteins—a comparative nonequilibrium molecular dynamics study. *Biophysical Journal, 119*(5), 939-949.
29. Patel, J. S., Berteotti, A., Ronsisvalle, S., Rocchia, W., & Cavalli, A. (2014). Steered molecular dynamics simulations for studying protein–ligand interaction in cyclin-dependent kinase 5. *Journal of chemical information and modeling, 54*(2), 470-480.
30. Phillips, J. C., Braun, R., Wang, W., Gumbart, J., Tajkhorshid, E., Villa, E., ... & Schulten, K. (2005). Scalable molecular dynamics with NAMD. *Journal of computational chemistry, 26*(16), 1781-1802.
31. Sánchez, W. N., Robeson, L., Carrasco, V., Figueroa, N. L., Burgos-Bravo, F., Wilson, C. A., & Casanova-Morales, N. (2022). Determination of protein–protein interactions at the single-molecule level using optical tweezers. *Quarterly Reviews of Biophysics, 55*, e8.
32. Tomarchio, R., Patamia, V., Zagni, C., Crocetti, L., Cilibrizzi, A., Floresta, G., & Rescifina, A. (2023). Steered molecular dynamics simulations study on FABP4 inhibitors. *Molecules, 28*(6), 2731.
33. Trizio, E., Rizzi, A., Piaggi, P. M., Invernizzi, M., & Bonati, L. (2024). Advanced simulations with PLUMED: OPES and machine learning collective variables. a*rXiv preprint arXiv:2410*.18019.
34. Wang, H., Guo, Y., Zou, R., Hu, H., Wang, Y., Wang, F., & Ju, L. A. (2022). Recent advances of optical tweezers–based dynamic force spectroscopy and mechanical measurement assays for live-cell mechanobiology. *Frontiers in Physics, 10,* 771111.
35. Wagoner, J. A., & Dill, K. A. (2021). Evolution of mechanical cooperativity among myosin II motors. *Proceedings of the National Academy of Sciences, 118(20)*, e2101871118.
36. Alston, J. J., Soranno, A., & Holehouse, A. S. (2021). Integrating single-molecule spectroscopy and simulations for the study of intrinsically disordered proteins. *Methods, 193*, 116-135.

Supplementary Materials

1. Scope and Purpose of the Supplemental Methods

The main manuscript proposes that the cardiomyopathy-associated R975W substitution in the metavinculin tail domain converts a positively charged arginine into a bulky hydrophobic tryptophan, producing a local hydrophobic patch and surface protrusion that may alter actin-binding geometry, weaken force-dependent metavinculin-actin bonding, and disrupt metavinculin control over vinculin-driven F-actin organization. The purpose of this supplement is to provide enough methodological detail for readers to reproduce, refine, or experimentally test that hypothesis using molecular modeling, molecular dynamics, steered molecular dynamics, enhanced sampling, and single molecule force spectroscopy. References are included in the main manuscript bibliography.

2. Structural Model Preparation

- Starting Structures: The metavinculin tail-domain model used in the manuscript should be retained as the primary model for the R975W structural comparison because the mutation is interpreted at the local surface and actin-regulatory interface level. When the full-length cryo-EM structure of human metavinculin is used for future simulations, unresolved loops or missing regions should be modeled explicitly before molecular dynamics. The original preliminary notes identified missing coordinates in the full-length 7KTT model in the regions 837–959 and 1117–1142; therefore, any full-length simulation should document how these segments were reconstructed.
- Sequence and Residue Consistency: Before introducing mutations, the SEQRES-derived full sequence, ATOM-coordinate residue numbering, and UniProt numbering should be crosschecked. This step is essential because metavinculin contains an isoform-specific insert in the tail domain, and incorrect residue mapping could shift R975 or neighboring residues. A table listing the PDB chain, sequence range, modeled region, missing residues, and final residue numbering should be retained as part of the reproducibility package.
- Mutation Generation: The R975W variant should be generated using a controlled mutagenesis workflow in PyMOL, Chimera/ChimeraX, or a comparable molecular-modeling package. Multiple tryptophan rotamers should be inspected, and the selected rotamer should minimize steric clashes while preserving the local backbone. If a structural minimization step is performed, both the unminimized and minimized mutant PDB files should be archived.
- Initial Structural Descriptors: The WT and R975W models should be compared using local solvent-accessible surface area, hydrophobic surface area near residue 975, electrostatic/hydrophobic surface coloring, local protrusion/shape change, residue contacts within 4–5 Å, and distances between R/W975 and nearby actin-facing residues. These descriptors support the manuscript's visual PyMOL observation and define quantitative variables for subsequent MD validation.

3. Preparation of Metavinculin-Actin Models for Simulation

The actin-bound model should be constructed from the best available vinculin/metavinculin-actin structural information and then refined to avoid unrealistic clashes at the actin-binding interface. The simulation system can use a short F-actin filament, such as five actin subunits, as described in the proposed workflow. To preserve filament geometry during pulling simulations, distal actin monomers may be restrained while central actin subunits remain free to interact with metavinculin. The final model should include WT metavinculin tail domain, R975W metavinculin tail domain, and, where relevant, additional cardiomyopathy-associated variants such as A934V and ΔL954 for comparison.

Item	Recommended Choice	Rationale	Output to Archive
Protein model	WT metavinculin tail and R975W mutant	Directly tests the manuscript hypothesis	WT.pdb, R975W.pdb
Actin model	Short F-actin filament, preferably five subunits	Maintains local filament geometry while limiting system size	actin_complex.pdb
Mutation control	Same preparation pipeline for WT and mutant	Avoids attributing preparation artifacts to mutation	preparation log
Numbering control	SEQRES/ATOM/UniProt mapping	Prevents residue-number mismatch	residue map table
Surface descriptors	SASA, hydrophobic patch, contacts, electrostatics	Quantifies PyMOL-level structural observation	analysis scripts and CSV

Table S1: Recommended Structural Model Preparation Outputs

4. Molecular Dynamics System Setup

All-atom MD simulations should be performed using an established biomolecular force field and standard explicit-solvent conditions. A consistent setup should be used for WT and R975W systems so that any difference in stability, contacts, or force response can be attributed to the mutation rather than to model preparation. The proposed workflow can be implemented in NAMD or a comparable MD engine, with PLUMED used for enhanced sampling where required.

Parameter	Suggested Implementation Detail	Reason for Reporting
Force field	CHARMM 36m, AMBER ff14SB/ff19SB, or another validated protein force field; use the same force field for all systems	Force field choice can affect protein flexibility and unbinding pathways
Solvent and ions	Explicit water, neutralizing ions, and physiological salt concentration such as 150 mM NaCl	Electrostatics are central to the Arg-to-Trp substitution hypothesis
Box padding	At least 1.0 nm water padding around the complex after solvation	Avoids protein-image interactions under periodic boundary conditions
Minimization	Energy minimization until the system is free of severe steric clashes	Ensures the R975W rotamer and local contacts are physically plausible
Equilibration	Restrained equilibration followed by unrestrained or weakly restrained equilibration at 310 K and 1 atm	Approximates physiological temperature and allows local relaxation
Production MD	Replicate simulations for WT and R975W before SMD/ enhanced sampling	Replicates help distinguish robust mutation effects from stochastic variation
Trajectory outputs	Coordinates, velocities if needed, energies, restraint files, topology, and parameter files	Allows independent reproduction of the workflow

Table S2: Recommended MD System Setup Details to Report

5. Steered Molecular Dynamics and Force-Coordinate Definition

Force-dependent behavior should be tested using SMD by applying controlled directional forces to the metavinculin-actin interface. The pulling direction must be defined relative to the actin filament axis rather than arbitrary Cartesian coordinates. Two collective variables can be used: $Q\parallel$, describing displacement along the actin filament, and $Q\perp$, describing displacement away from the filament surface. This matches the manuscript's focus on direction-dependent mechano transduction. For constant-force simulations, forces from -30 to +30 pN can be tested in both WT and R975W models, consistent with the proposed physiological-force framework. For constant-velocity pulling, pulling speed, spring constant, anchor atoms, pulled atom groups, and restrained actin subunits must be explicitly reported. In either mode, the same atom selection and coordinate definition should be used for WT and R975W.

6. Enhanced Sampling and Free-Energy Analysis

Standard MD may not efficiently observe protein unbinding or rare conformational transitions. Therefore, enhanced sampling should be used to estimate the free-energy landscape of WT and R975W metavinculin-actin models. OPES-MetaD can be used to estimate free-energy surfaces along $Q\parallel$ and $Q\perp$, while OPES-flooding or related rate-focused approaches can be used to estimate unbinding lifetimes. For each calculation, the final supplement or deposited computational protocol should report collective variables, bias parameters, simulation length, number of independent replicas, convergence diagnostics, and error estimates.

7. Recommended Analysis Readouts

Readout	What to compare	Interpretation if R975W is disruptive	Recommended output
Local hydrophobic surface area	WT versus R975W near residue 975	Increase supports the hydrophobic-patch mechanism	surface area table, PyMOL/Chimera sessiona
Residue contacts and salt bridges	Contacts around residue 975 and actin-facing residues	Loss or rearrangement suggests altered binding geometry	contact maps
RMSD/RMSF	Global and local flexibility of tail domain	Higher local flexibility may indicate destabilized interface	trajectory plots
Buried surface area	Metavinculin-actin interface under load	Reduced BSA suggests weakened binding	BSA versus time plot
Free-energy barrie	WT and R975W FES along Q variables	Lower barrier in mutant suggests weaker thermodynamic stability	FES maps
Unbinding lifetime	Lifetime versus force curve	Loss of catch-bond-like strengthening supports impaired mechanotransduction	force-lifetime plot
Rupture force	WT versus R975W under identical SMD Protocol	Lower rupture force suggests weaker mechanical coupling	rupture-force distribution

Table S3: Recommended Analysis Readouts for Testing the R975W Hypothesis

8. Single-Molecule Force Spectroscopy Validation

The computational hypothesis should ideally be validated by single-molecule force spectroscopy using an optical-trap or equivalent dynamic force spectroscopy platform. Recombinant WT and R975W metavinculin tail-domain constructs should be expressed, purified, and site-specifically biotinylated where possible. F-actin should be immobilized in a geometry that allows directional force application. A bead carrying the metavinculin construct can be brought into contact with F-actin, force-clamped, and monitored until bond rupture. The primary measured variable is the unbinding lifetime as a function of applied force. A WT curve that increases in lifetime under moderate force would be consistent with catch-bond-like reinforcement, whereas a flattened or shortened R975W force-lifetime curve would support the hypothesis that R975W compromises force-dependent bonding.

9. Minimum Reproducibility Package

- WT and R975W PDB files before and after minimization.
- Residue-numbering map showing correspondence among PDB, modeled construct, and canon-ical metavinculin sequence.
- PyMOL/Chimera session files or scripts used to generate structural figures.
- MD topology, coordinate, force-field, restraint, and run-parameter files.
- PLUMED input files for Q□, Q□, OPES-MetaD, and OPES-flooding analyses.
- Analysis scripts for RMSD/RMSF, contact maps, BSA, hydrophobic surface area, FES, rupture-force extraction, and lifetime fitting.
- Raw and processed force-spectroscopy traces if experimental validation is performed.

10. Database/Web Server Statement

Not applicable. This manuscript does not describe a new or updated database, web server, online resource, or hosted software tool. The work is a short structural hypothesis/communication supported by PyMOL-based preliminary structural comparison and a proposed validation strategy using MD, SMD, enhanced sampling, and single-molecule force spectroscopy.

11. References Cited in this Supplemental Material

References cited in this supplemental material are included in the main manuscript reference list.